

Supporting Information for

A Breast Cancer Stem Cell Selective, Mammospheres Potent Osmium(VI) Nitrido Complex

Kogularamanan Suntharalingam,[†] Wei Lin,[†] Timothy C. Johnstone,[†] Peter M. Bruno,[‡] Yao-Rong Zheng,[†] Michael T. Hemann,[‡] and Stephen J. Lippard^{†*}

[†]Department of Chemistry, Massachusetts Institute of Technology, Cambridge, Massachusetts 02139, United States

[‡]The Koch Institute for Integrative Cancer Research, Massachusetts Institute of Technology, Cambridge, Massachusetts, 02139, United States

Email: lippard@mit.edu

Content

Experimental Details

- Figure S1. UV-vis spectrum of **1** (80 μ M) in MEGM cell media over the course of 72 h at 25 °C.
- Figure S2. (a) 2-D plot displaying side-scattered light (SSC) versus the red fluorescence emitted by anti-CD44-APC antibody stained HMLER cells (red dots) and HMLER^{tax} cells (blue dots) (FL-4) (b) Histograms displaying the red fluorescence emitted by anti-CD44-APC antibody stained HMLER cells (red line) and HMLER^{tax} cells (blue line). In this example, HMLER cells contain ~7% CD44^{high} cells and HMLER^{tax} contain ~54% CD44^{high} cells.
- Figure S3. Average dose-response curves for the treatment of HMLER and HMLER^{tax} cells with **2** (n = 18 for each point).
- Figure S4. Average dose-response curves for the treatment of HMLER and HMLER^{tax} cells with **3** (n = 18 for each point).
- Figure S5. Average dose-response curves for the treatment of HMLER and HMLER^{tax} cells with salinomycin (n = 30 for each point).
- Figure S6. Average dose-response curves for the treatment of HMLER and HMLER^{tax} cells with abamectin (n = 30 for each point).
- Figure S7. Average dose-response curves for the treatment of HMLER and HMLER^{tax} cells with cisplatin (n = 30 for each point).
- Figure S8. Average dose-response curves for the treatment of HMLER and HMLER^{tax} cells with carboplatin (n = 30 for each point).
- Figure S9. Average dose-response curves for the treatment of HMLER and HMLER^{tax} cells with oxaliplatin (n = 30 for each point).
- Figure S10. Average dose-response curves for the treatment of HMLER and HMLER^{tax} cells with satraplatin (n = 30 for each point).
- Figure S11. Average dose-response curves for the treatment of HMLER and HMLER^{tax} cells with **Pt(IV)-C2** (n = 18 for each point).

- Figure S12. Average dose-response curves for the treatment of HMLER and HMLER^{tax} cells with **Pt(IV)-C16** (n = 18 for each point).
- Figure S13. Representative histograms displaying the red fluorescence emitted by anti-CD44-APC antibody stained HMLER cells (red) and HMLER cells treated with **1** (5 μ M, blue; 10 μ M, orange; 20 μ M, light green; 40 μ M, dark green) for 4 days followed by 4 days recovery in compound-free MEGM media.
- Figure S14. Representative histograms displaying the red fluorescence emitted by anti-CD44-APC antibody stained HMLER cells (red), HMLER^{tax} cells (blue) and HMLER^{tax} cells treated with cisplatin (1.5 μ M, orange), carboplatin (15 μ M, light green), oxaliplatin (15 μ M, dark green) and satraplatin (1.5 μ M, brown) for 4 days followed by 4 days recovery in compound-free MEGM media.
- Figure S15. Representative histograms displaying the red fluorescence emitted by anti-CD44-APC antibody stained HMLER cells (red) and HMLER cells treated with cisplatin (1.5 μ M, blue), carboplatin (15 μ M, orange), oxaliplatin (15 μ M, light green) and satraplatin (1.5 μ M, dark green) for 4 days followed by 4 days recovery in compound-free MEGM media.
- Figure S16. Representative 3D representations of the mammospheres formed using HMLER breast cancer cells, untreated (A) and treated with paclitaxel (B), salinomycin (C), **1** (D), cisplatin (E), carboplatin (F), oxaliplatin (G), and satraplatin (H) (at their respective IC₃₀ values for 5 days). The images show the overlay of Hoechst 33258 (blue) and APC labelled anti-CD44 antibody (red) fluorescence.
- Figure S17. Quantification of secondary mammosphere formation from untreated primary mammospheres and **1**-, salinomycin-, paclitaxel-treated primary mammospheres (at their respective IC₃₀ values). Student *t-test*, p < 0.01. Error bars represent standard deviations.
- Figure S18. Immunoblotting analysis of proteins related to the DNA damage pathway, ER stress pathway and apoptosis pathway. Protein expression in HMLER cells following treatment with **1** (5–20 μ M) after 72 h incubation. Whole cell lysates were resolved by SDS-PAGE and analyzed by immunoblotting against γ H2AX, phos-CHK2, phos-eIF2 α , CHOP, p21, cleaved caspase 7, cleaved caspase 3, cleaved PARP-1, and β -actin (loading control).
- Figure S19. Immunofluorescence staining analysis of the phosphorylated PERK protein in HMLER breast cancer cells, untreated (A & D) and treated with **1** (25 μ M for 24 h) (B & E), thapsigargin (0.25 μ M for 24 h) (C & F). The images show the overlay of Hoechst 33258 (blue) and FITC fluorescence (green) corresponding to phosphorylated PERK expression.
- Figure S20. Graphical representation of the IC₅₀ values of **1** against HMLER and HMLER^{tax} cells in the absence and presence of ER stress inhibitor, salubrinal (10 μ M). Student *t-test*, p < 0.05. Error bars represent standard deviations.

Experimental Details

Materials and Methods. Cisplatin was obtained from Strem Chemicals. Carboplatin, oxaliplatin, satraplatin, and **1** were prepared according to reported protocols.¹⁻⁵ Salinomycin and abamectin were purchased from commercial vendors and used as received. The structural integrity of the compounds was confirmed by ¹H NMR spectroscopy prior to use.

Cell Lines and Cell Culture Conditions. The human mammary epithelial cell line, HMLER, was kindly donated by Prof. R. A. Weinberg (Whitehead Institute, MIT). HMLER cells were maintained in Mammary Epithelial Cell Growth Medium (MEGM) with supplements and growth factors (BPE, hydrocortisone, hEGF, insulin, and gentamicin/amphotericin-B). The cells were grown at 37 °C in a humidified atmosphere containing 5% CO₂. HMLER^{tax} cells were generated by incubating HMLER cells with paclitaxel (10 nM) for 4 days, followed by 4 days of incubation in paclitaxel-free media.

Cytotoxicity MTT assay. The colorimetric MTT assay was used to determine the toxicity of **1**, **2**, **3**, salinomycin, abamectin, cisplatin, carboplatin, oxaliplatin, satraplatin, **Pt(IV)-C2**, and **Pt(IV)-C16**. HMLER (3×10^3) or HMLER^{tax} cells (5×10^3) were seeded in each well of a 96-well plate. After incubating the cells overnight, various concentrations of the compounds, as determined by GF-AAS or UV-vis spectroscopy (0.3-100 μM), were added and incubated for 72 h (total volume 200 μL). Stock solutions of the compounds were prepared as 1-2 mM solutions in ddH₂O or DMSO and diluted using media. The final concentration of DMSO in each well was 0.5% and this amount was present in the untreated control as well. After 72 h, the medium was removed, 200 μL of a 0.4 mg/mL solution of MTT in MEGM was added, and the plate was incubated for an additional 4 h. The MEGM/MTT mixture was aspirated and 200 μL of DMSO was added to dissolve the resulting purple formazan crystals. The absorbance of the solution in each well was read at 550 nm. Absorbance values were normalized to DMSO-containing control wells and plotted as concentration of test compound versus % cell viability. IC₅₀ values were interpolated from the resulting dose dependence curves. The reported IC₅₀ values are the average of three or five independent experiments, each of which consisted of six replicates per concentration level (overall n = 18 or 30). For probing the ER stress pathway, the ER stress inhibitor, salubrinal (10 μM) was added to HMLER and HMLER^{tax} cells prior to treatment with the test compounds.

Flow cytometry. HMLER or HMLER^{tax} cells were seeded in 6-well plates at a density of 5×10^5 cells/mL and the cells were allowed to attach overnight. The cells were then treated with cisplatin (1.5 μM), carboplatin (15 μM), oxaliplatin (15 μM), satraplatin (1.5 μM), or **1** (5-40 μM) and incubated for 4 days. The compound-containing medium was then removed and replaced with fresh medium and incubated for an additional 4 days. The cells were harvested by trypsinization and suspended in PBS (200 μL). The APC labelled anti-CD44 antibody (15 μL) was then added to the cell suspension, which was subsequently incubated in the dark for 20 min. The cells were analyzed using a FACSCalibur-HTS flow cytometer (BD Biosciences) (20,000 events per sample were acquired). The FL4 channel was used to assess CD44 expression. Cell populations were analyzed using the FlowJo software (Tree Star).

Tumorsphere formation assay. HMLER cells (3×10^5) were plated in ultralow-attachment culture plates (Corning) and incubated in MEGM supplemented with B27 (Invitrogen), 20 ng/mL EGF, and 4 μg/mL heparin (Sigma) for 5 days. Studies were also conducted in the presence of **1**, salinomycin, paclitaxel, cisplatin, carboplatin, oxaliplatin, and satraplatin (at their respective IC₃₀ values). Mammospheres were counted using an inverted microscope. In order to obtain three-dimensional images and to determine the proportion of CD44-positive

cells within a given mammosphere, cells were incubated with the nuclear staining dye, Hoechst 33258 dye (7.5 μ M for 30 min), and the APC labelled anti-CD44 antibody (15 μ L for 45 min) respectively, and imaged using a Zeiss Axiovert 200M inverted epifluorescence microscope with a Hamamatsu EM-CCD digital camera C9100 and a MS200 XY Piezo Z stage (Applied Scientific Instruments, Inc.). An XCite 120 metal halide lamp (EXFO) was used as the light source. Zeiss standard filter sets 49 and 43 HE were employed for imaging Hoechst 33258 and APC. The microscope was operated with Volocity software (version 6.01, Improvion). The exposure time for acquisition of fluorescence images was kept constant for each series of images at each channel. Fluorescence images were deconvoluted using Volocity restoration algorithms. Z-sectioned images were obtained at 1 μ m intervals in a 160 μ m range to give three-dimensional images of the mammospheres. The proportion of CD44-positive cells within a given mammosphere was estimated by quantification of the mean APC fluorescence using Volocity software (version 6.01, Improvion). To do so, the whole mammosphere was selected as the region of interest. The integrated fluorescence from the background region was subtracted from the integrated fluorescence intensity of the region of interest.

Secondary tumorsphere formation assay. 1-, salinomycin-, and paclitaxel-treated HMLER mammospheres were dissolved into single-cell suspensions by trypsinization. These single-cells (2×10^5) were plated in ultralow-attachment culture plates (Corning) and incubated in MEGM supplemented with B27 (Invitrogen), 20 ng/mL EGF, and 4 μ g/mL heparin (Sigma) for 5 days. After this period, mammospheres were counted using an inverted microscope at 4x magnification.

RNAi Signatures. Compounds were dosed to achieve an LD₈₀₋₉₀ in *E μ -Mycp19arf*^{-/-} cells by propidium iodide exclusion as determined by FACS after a 48 h incubation. GFP enrichment/depletion was then determined by FACS at 72 h. Linkage ratios (LR) and p-values were generated as previously reported.⁶⁻⁸ All FACS was conducted using a FACScan (BD Biosciences).

GFP Competition assays. *E μ -Mycp19arf*^{-/-} lymphoma or p185+ *BCR-Abl*^{p19arf}^{-/-} leukemia cells were infected with GFP-tagged shRNAs such that 15-25% of the population were GFP positive. An eighth of a million cells in 250 μ L B-cell media (BCM) were then seeded into 24-well plates. For wells that would remain untreated as a control, only 1/16th of a million cells were seeded. Next, 250 μ L of media containing the active agent was added to the cells. After 24 h, 300 μ L of cells from untreated wells are removed and replaced by 300 μ L fresh BCM. All wells then received 500 μ L BCM before being placed by in the incubator for another 24 h. At 48 h, cells transduced with the control vector, MLS, were checked for viability via FACS on a FACScan (BD Biosciences) using propidium iodide as a live/dead marker. Untreated wells then had 700 μ L of cells removed and replaced with 700 μ L fresh media followed by a further 1 mL of fresh media. Wells for which the compound had killed 80-90% of cells (LD₈₀₋₉₀) were then diluted further by adding 1 mL of BCM. Finally, at 72 h, all wells for which an LD₈₀₋₉₀ was achieved, as well as the untreated samples, were analyzed via FACS to determine GFP% enrichment.

PCA methods. Principal components analysis (PCA) was performed using the princomp.m function in MATLAB 2013b. The input matrix consisted of the variables, the eight shRNAs, in each column and the observations, the drugs, in each row. All observations from the input matrix were plotted on the first two principal components.

Immunoblotting Analysis. HMLER cells (5×10^5 cells) were incubated with **1** (5-20 μM) for 72 h at 37 $^\circ\text{C}$. Cells were washed with PBS, scraped into SDS-PAGE loading buffer (64 mM Tris-HCl (pH 6.8)/ 9.6% glycerol/ 2% SDS/ 5% β -mercaptoethanol/ 0.01% Bromophenol Blue), and incubated at 95 $^\circ\text{C}$ for 10 min. Whole cell lysates were resolved by 4-20 % sodium dodecylsulphate polyacrylamide gel electrophoresis (SDS-PAGE; 200 V for 25 min) followed by electro transfer to polyvinylidene difluoride membrane, PVDF (350 mA for 1 h). Membranes were blocked in 5% (w/v) non-fat milk in PBST (PBS/ 0.1% Tween 20) and incubated with the appropriate primary antibodies (Cell Signalling Technology and Santa Cruz). After incubation with horseradish peroxidase-conjugated secondary antibodies (Cell Signalling Technology), immune complexes were detected with the ECL detection reagent (BioRad) and analyzed using an Alpha Innotech ChemiImagerTM 5500 fitted with a chemiluminescence filter.

Immunofluorescence. HMLER cells (1×10^4 cells) were incubated with **1** (20 μM) or thapsigargin (0.25 μM) for 24 h at 37 $^\circ\text{C}$. The cells were then washed with PBS (2 mL \times 2) and fixed with 4% paraformaldehyde in PBS. The fixed cells were blocked in 5% goat serum and 0.3% Triton X-100 in PBS and incubated with the phosphorylated PERK-specific primary antibody (Cell Signalling Technology). After incubation with the corresponding FITC-conjugated secondary antibody, the cells were imaged using an inverted epifluorescence microscope.

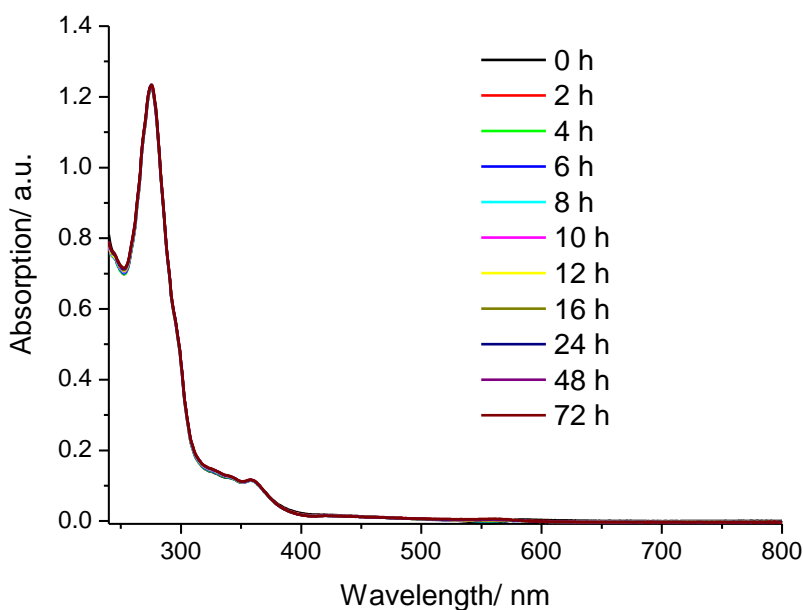


Figure S1. UV-vis spectrum of **1** (80 μM) in MEGM cell media over the course of 72 h at 25 $^\circ\text{C}$.

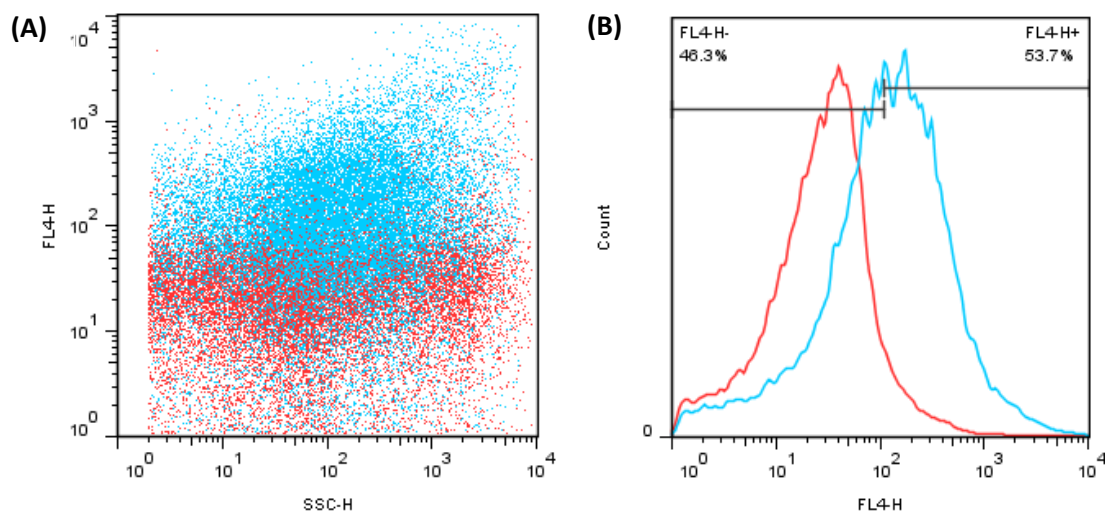


Figure S2. (a) 2-D plot displaying side-scattered light (SSC) versus the red fluorescence emitted by anti-CD44-APC antibody stained HMLER cells (red dots) and HMLER^{tax} cells (blue dots) (FL-4) (b) Histograms displaying the red fluorescence emitted by anti-CD44-APC antibody stained HMLER cells (red line) and HMLER^{tax} cells (blue line). In this example, HMLER cells contain ~7% CD44^{high} cells and HMLER^{tax} contain ~54% CD44^{high} cells.

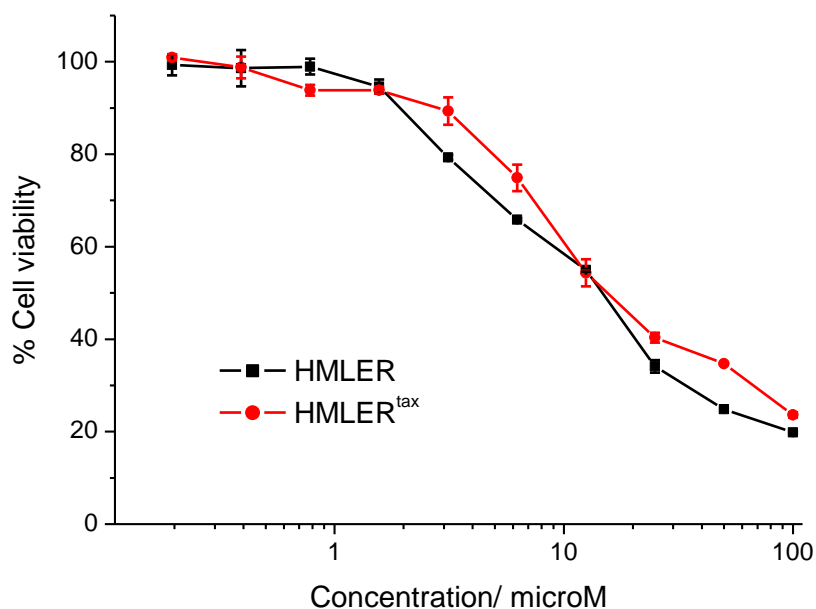


Figure S3. Average dose-response curves for the treatment of HMLER and HMLER^{tax} cells with **2** (n = 18 for each point).

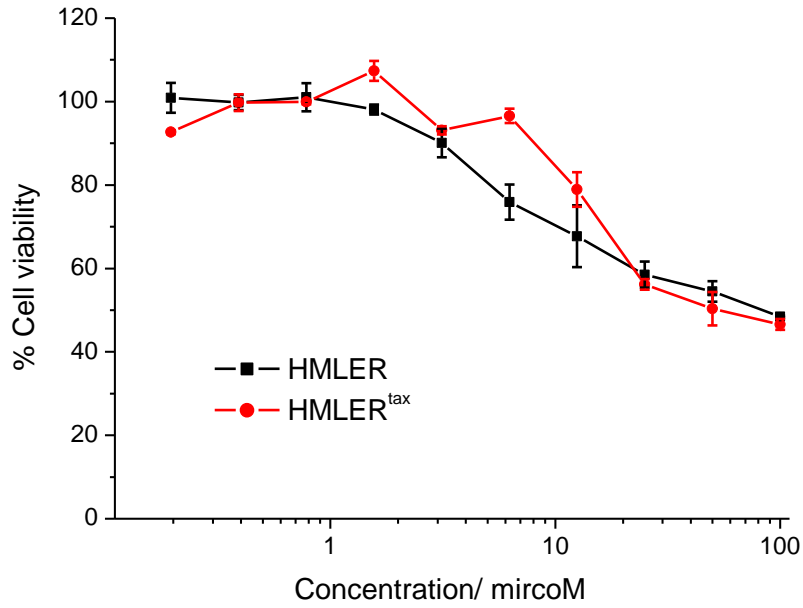


Figure S4. Average dose-response curves for the treatment of HMLER and HMLER^{tax} cells with **3** (n = 18 for each point).

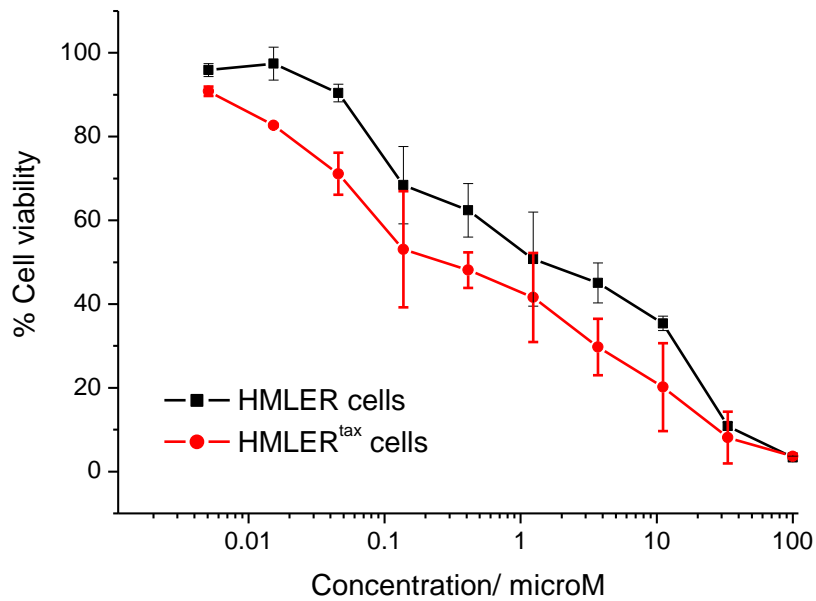


Figure S5. Average dose-response curves for the treatment of HMLER and HMLER^{tax} cells with salinomycin (n = 30 for each point).

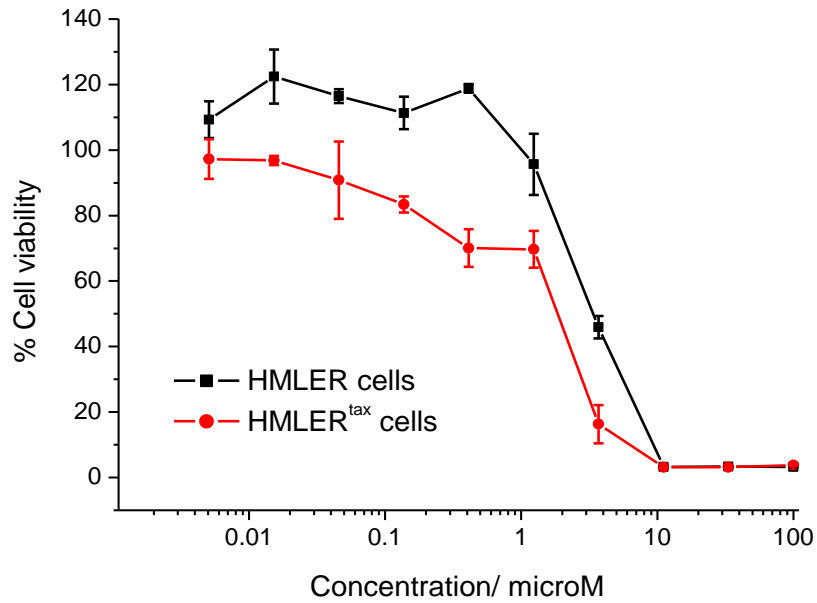


Figure S6. Average dose-response curves for the treatment of HMLER and HMLER^{tax} cells with abamectin (n = 30 for each point).

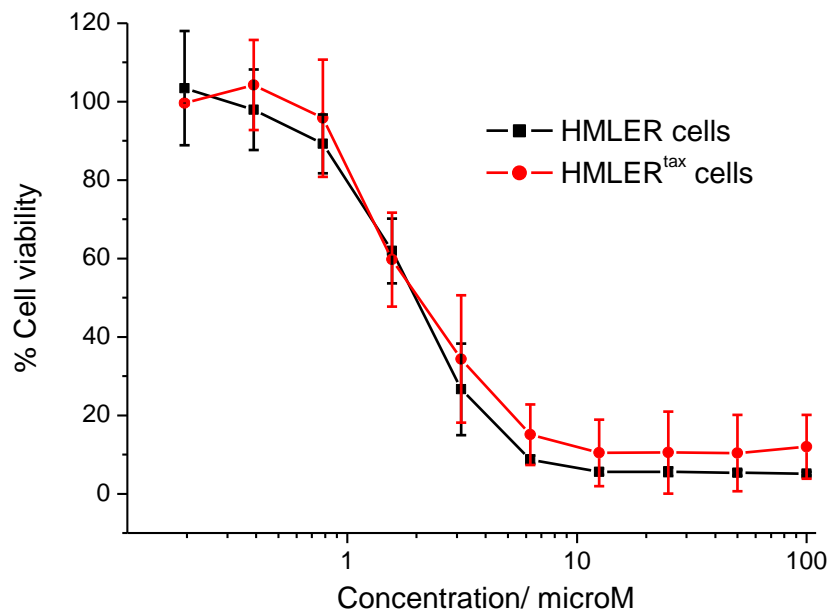


Figure S7. Average dose-response curves for the treatment of HMLER and HMLER^{tax} cells with cisplatin (n = 30 for each point).

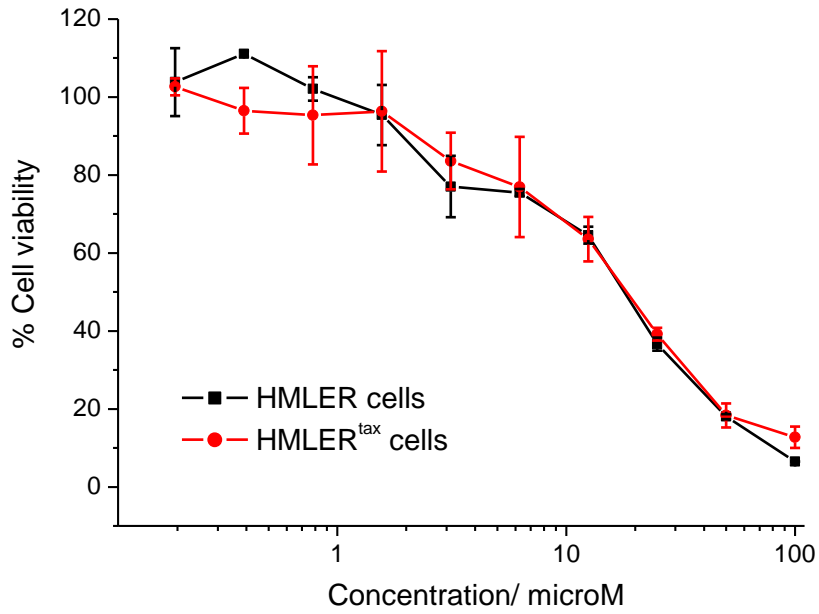


Figure S8. Average dose-response curves for the treatment of HMLER and HMLER^{tax} cells with carboplatin (n = 30 for each point).

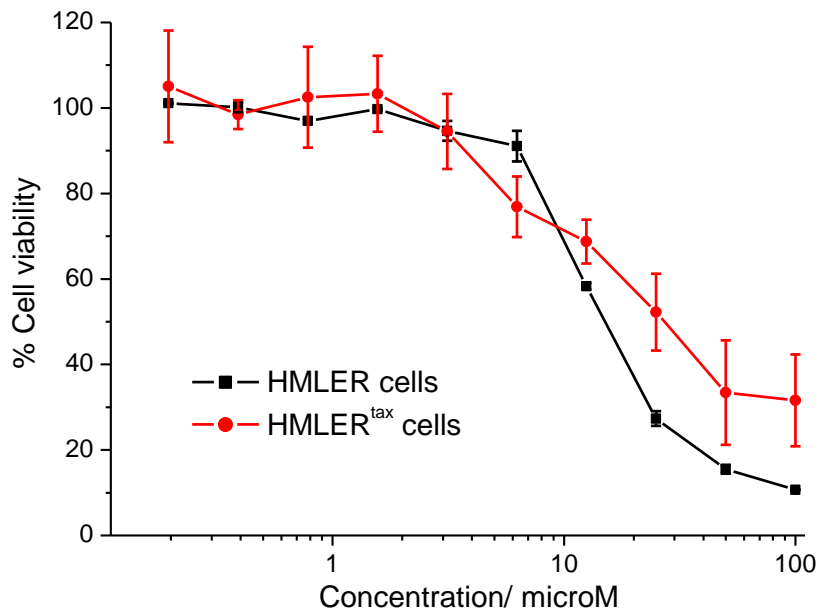


Figure S9. Average dose-response curves for the treatment of HMLER and HMLER^{tax} cells with oxaliplatin (n = 30 for each point).

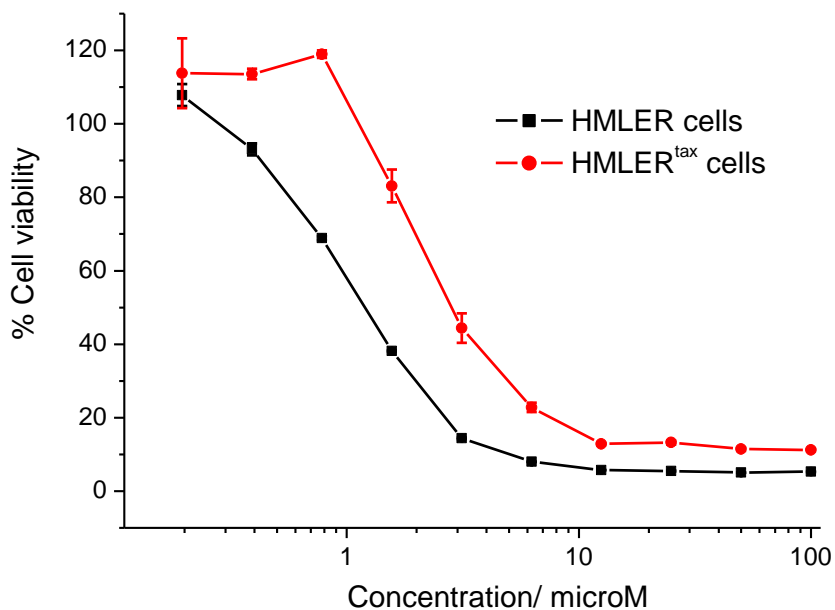


Figure S10. Average dose-response curves for the treatment of HMLER and HMLER^{tax} cells with satraplatin (n = 30 for each point).

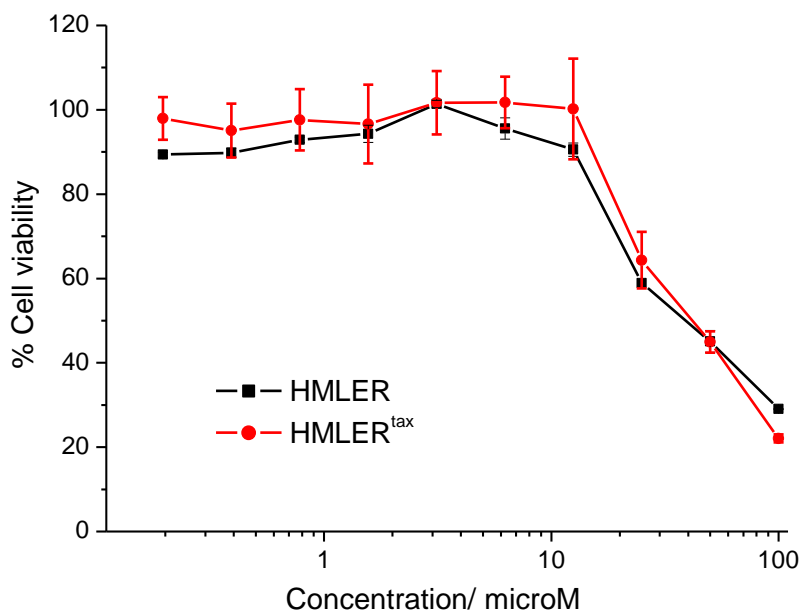


Figure S11. Average dose-response curves for the treatment of HMLER and HMLER^{tax} cells with Pt(IV)-C2 (n = 18 for each point).

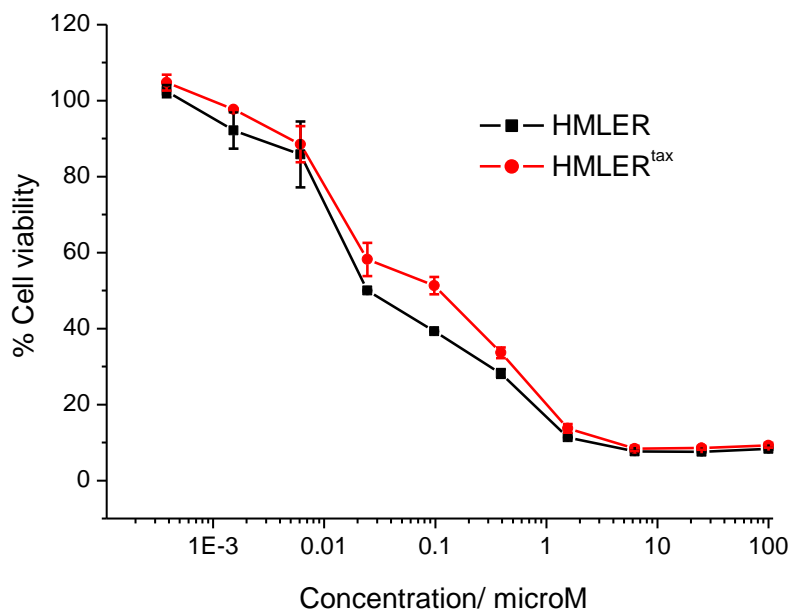


Figure S12. Average dose-response curves for the treatment of HMLER and HMLER^{tax} cells with Pt(IV)-C16 (n = 18 for each point).

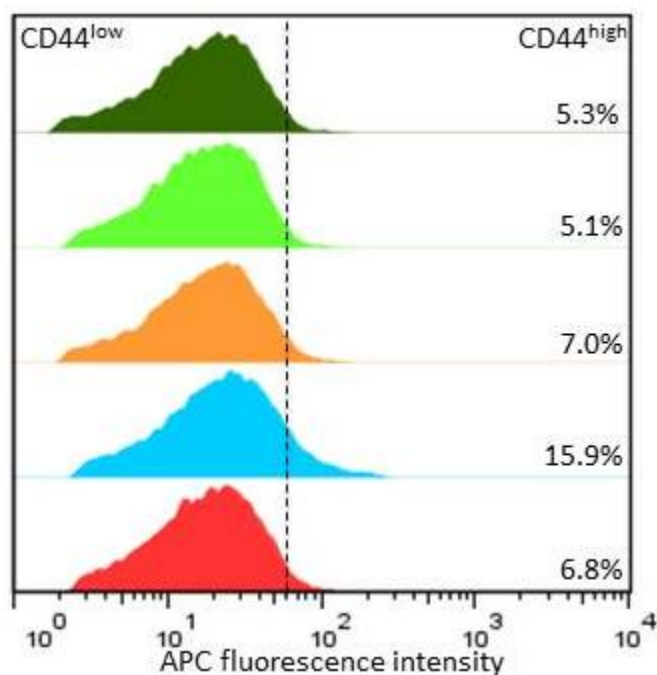


Figure S13. Representative histograms displaying the red fluorescence emitted by anti-CD44-APC antibody stained HMLER cells (red) and HMLER cells treated with **1** (5 μM, blue; 10 μM, orange; 20 μM, light green; 40 μM, dark green) for 4 days followed by 4 days of recovery in compound-free MEGM media.

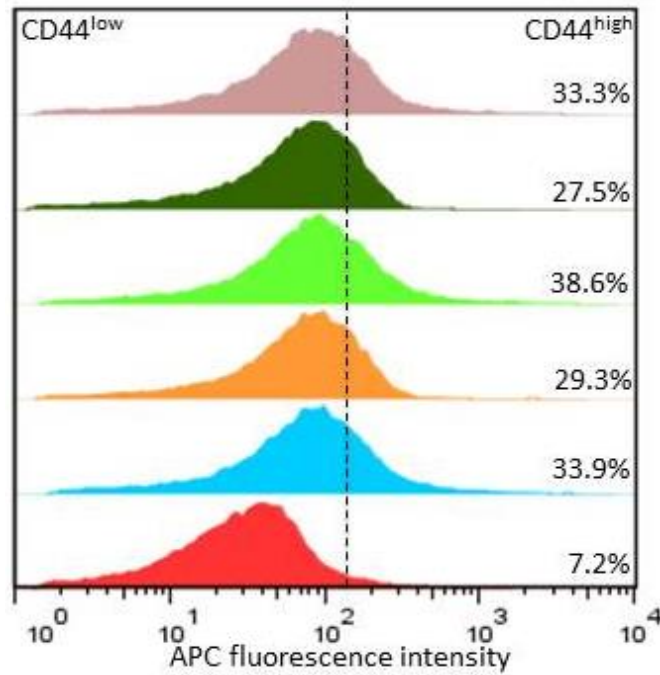


Figure S14. Representative histograms displaying the red fluorescence emitted by anti-CD44-APC antibody stained HMLER cells (red), HMLER^{tax} cells (blue) and HMLER^{tax} cells treated with cisplatin (1.5 μM, orange), carboplatin (15 μM, light green), oxaliplatin (15 μM, dark green), and satraplatin (1.5 μM, brown) for 4 days followed by 4 days of recovery in compound-free MEGM media.

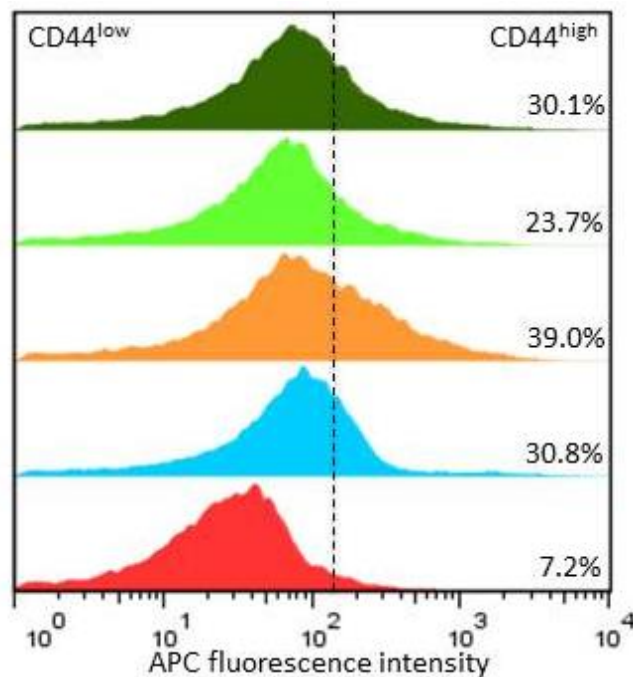


Figure S15. Representative histograms displaying the red fluorescence emitted by anti-CD44-APC antibody stained HMLER cells (red) and HMLER cells treated with cisplatin (1.5 μM, blue), carboplatin (15 μM, orange), oxaliplatin (15 μM, light green), and satraplatin (1.5 μM, dark green) for 4 days followed by 4 days of recovery in compound-free MEGM media.

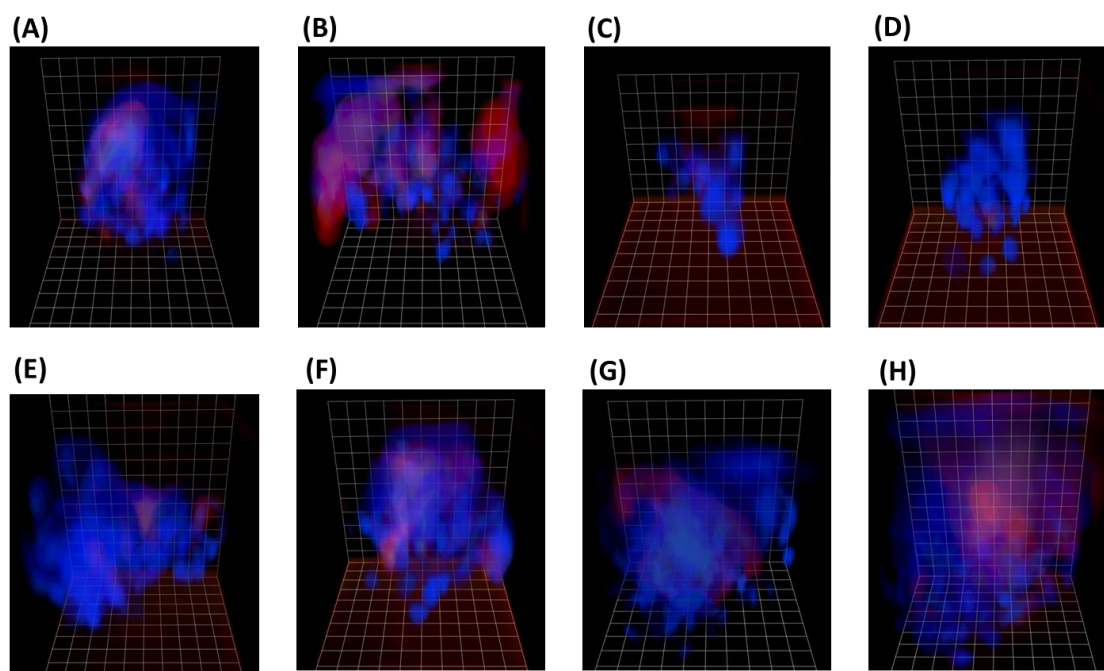


Figure S16. Representative 3D representations of the mammospheres formed using HMLER breast cancer cells, untreated (A) and treated with paclitaxel (B), salinomycin (C), **1** (D), cisplatin (E), carboplatin (F), oxaliplatin (G), and satraplatin (H) (at their respective IC_{30} values for 5 days). The images show the overlay of Hoechst 33258 (blue) and APC labelled anti-CD44 antibody (red) fluorescence.

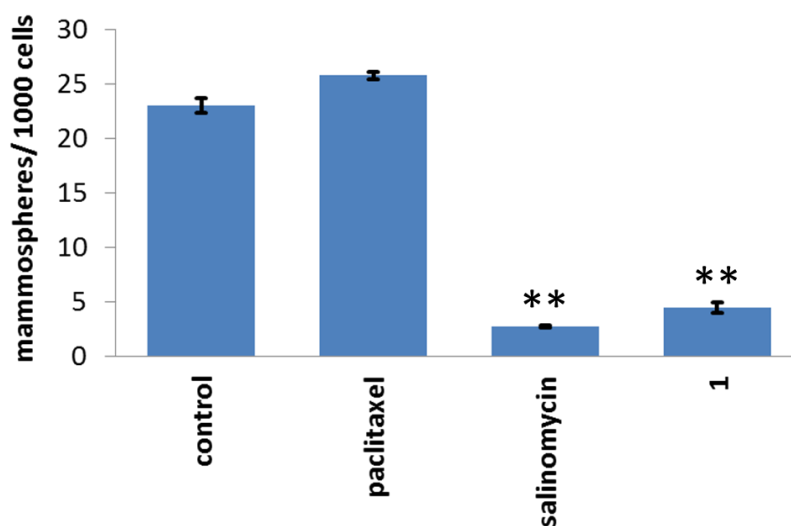


Figure S17. Quantification of secondary mammosphere formation from untreated primary mammospheres and **1**-, salinomycin-, paclitaxel-treated primary mammospheres (at their respective IC_{30} values). Student *t*-test, $p < 0.01$. Error bars represent standard deviations.

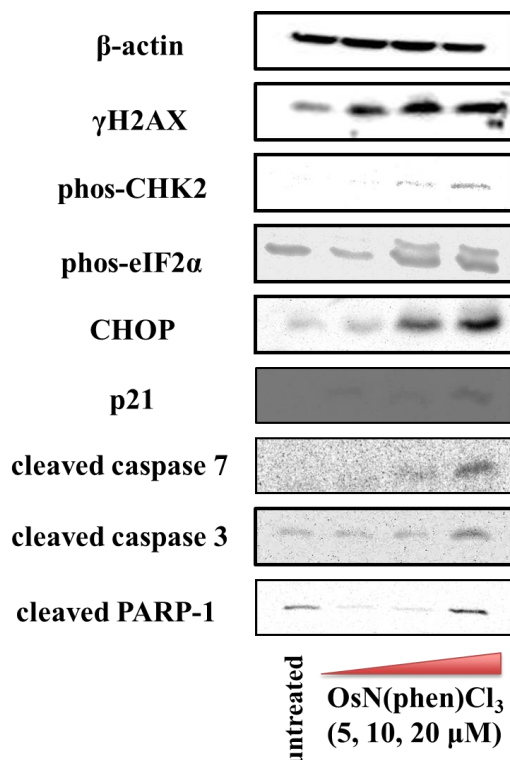


Figure S18. Immunoblotting analysis of proteins related to the DNA damage pathway, ER stress pathway and apoptosis pathway. Protein expression in HMLER cells following treatment with **1** (5–20 μM) after 72 h incubation. Whole cell lysates were resolved by SDS-AGE and analyzed by immunoblotting against γH2AX, phos-CHK2, phos-eIF2α, CHOP, p21, cleaved caspase 7, cleaved caspase 3, cleaved PARP-1, and β-actin (loading control).

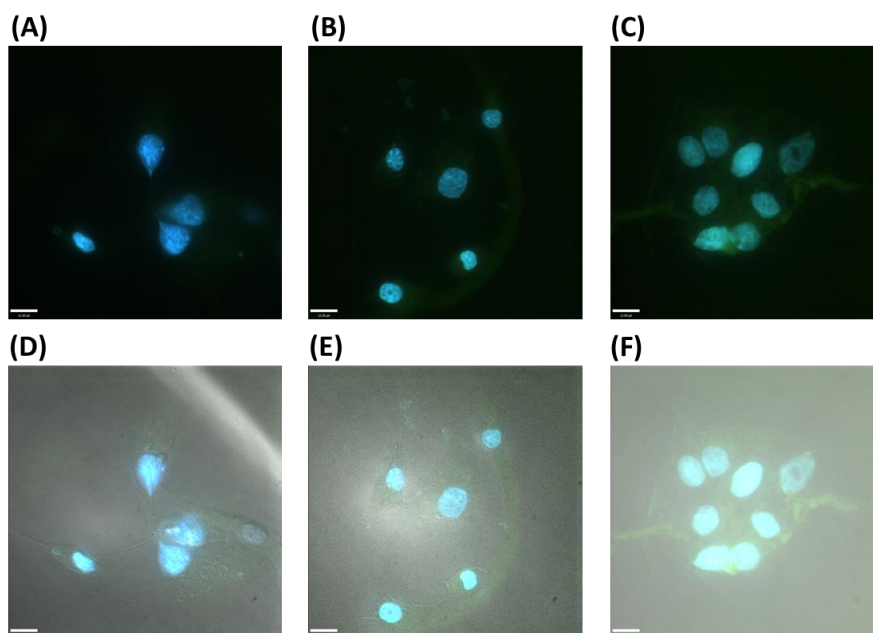


Figure S19. Immunofluorescence staining analysis of the phosphorylated PERK protein in HMLER breast cancer cells, untreated (A & D) and treated with **1** (25 μM for 24 h) (B & E), thapsigargin (0.25 μM for 24 h) (C & F). The images show the overlay of Hoechst 33258 (blue) and FITC fluorescence (green) corresponding to phosphorylated PERK expression.

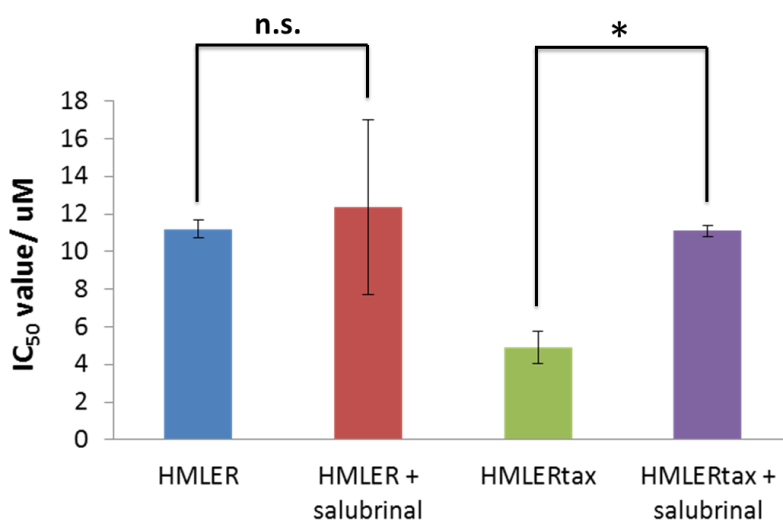


Figure S20. Graphical representation of the IC₅₀ values of **1** against HMLER and HMLER^{tax} cells in the absence and presence of ER stress inhibitor, salubrinal (10 μM). Student *t*-test, *p* < 0.05. Error bars represent standard deviations.

References

- (1) Giandomenico, C. M.; Abrams, M. J.; Murrer, B. A.; Vollano, J. F.; Rheinheimer, M. I.; Wyer, S. B.; Bossard, G. E.; Higgins, J. D. *Inorg. Chem.* **1995**, *34*, 1015.
- (2) Kidani, Y.; Inagaki, K.; Iigo, M.; Hoshi, A.; Kuretani, K. *J. Med. Chem.* **1978**, *21*, 1315.
- (3) Rochon, F. D.; Gruia, L. M. *Inorg. Chim. Acta* **2000**, *306*, 193.
- (4) Suntharalingam, K.; Johnstone, T. C.; Bruno, P. M.; Lin, W.; Hemann, M. T.; Lippard, S. J. *J. Am. Chem. Soc.* **2013**, *135*, 14060.
- (5) Zheng, Y. R.; Suntharalingam, K.; Johnstone, T. C.; Yoo, H.; Lin, W.; Brooks, J. G.; Lippard, S. J. *J Am Chem Soc* **2014**, *136*, 8790.
- (6) Jiang, H.; Pritchard, J. R.; Williams, R. T.; Lauffenburger, D. A.; Hemann, M. T. *Nat. Chem. Biol.* **2011**, *7*, 92.
- (7) Pritchard, J. R.; Bruno, P. M.; Gilbert, L. A.; Capron, K. L.; Lauffenburger, D. A.; Hemann, M. T. *Proc. Natl. Acad. Sci. U. S. A.* **2013**, *110*, E170.
- (8) Pritchard, J. R.; Bruno, P. M.; Hemann, M. T.; Lauffenburger, D. A. *Mol. BioSyst.* **2013**, *9*, 1604.